2012

A Homogeneous Capillary Tube Model - Comprehensive Parameter Studies Using Isobutane As Refrigerant

Martin Heimel
martin.heimel@tugraz.at

Wolfgang Lang

Erwin Berger

Raimund Almbauer

A Homogenous Capillary Tube Model - Comprehensive Parameter Studies Using R600a

Martin HEIMEL[1]*, Wolfgang LANG[2], Erwin BERGER[3], Raimund ALMBAUER[4]

[1, 2, 3, 4]Institute for Internal Combustion Engines and Thermodynamics, Graz University of Technology, Inffeldgasse 25/C, 8010 Graz, Austria

[1]*Heimel@ivt.tugraz.at,   +43 316 873 4776
[2]Wolfgang.Lang@ivt.tugraz.at, +43 316 873 4775
[3]Berger@ivt.tugraz.at,   +43 316 873 4580
[4]Almbauer@ivt.tugraz.at,   +43 316 873 7583

ABSTRACT

In this work a homogenous capillary tube model using R600a (isobutane) as refrigerant is presented. The capillary tube model underlies common restrictions; it is assumed to be adiabatic, straight with constant cross section and operates under steady state conditions. Different empirical correlations for friction and two-phase-viscosity are applied, and the resulting mass flow rates for given boundary conditions are compared with experimental data, available in open literature. The computational scheme comprises cell-wise iterative solution of conservation equations for mass, momentum and energy on a non-uniform, one-dimensional grid. Invariability-studies follow, where the number of computational cells is varied and the impact on the mass flow is investigated. In a next step, parameter variations of length, diameter, wall roughness, subcooling, inlet pressure, outlet pressure, friction laws, viscosity relations and the influence of gravity are investigated under different working conditions (choked and non-choked) with respect to the mass flow.

1. INTRODUCTION AND REVIEW

Capillary tubes are commonly used expansion devices in domestic refrigeration processes, where the use of electronically operated devices may be too costly in terms of money and effort. Its main advantages are its simplicity and the fact that this device is cheaper compared to any other realizable method. Also, it allows equalisation of the high- and low-pressure side during off-cycles to lower the starting torque of the motor (Peixoto and Bullard, 1994), which leads adversely to losses during the start-up. A capillary tube 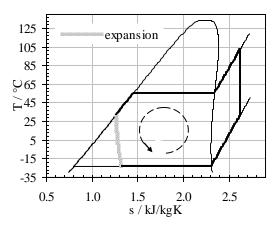basically is a small bore tube made of drawn copper with typical dimensions ranging somewhere between 1 and 5 meters in length and 0.5 up to 2 millimetres as inner diameter (Bansal and Rupasinghe, 1996), (Fang, 1999). The word "capillary" itself in this context might be misleading since the tube has little to do with the capillary effect, which causes a fluid to rise against gravity due to forces between the wall and the fluid. The main principle of a capillary tube is summarized quickly. Positioned between the condenser (high pressure) and the evaporator (low pressure) subcooled liquid refrigerant enters the capillary and reaches, after a certain pressure drop, its point of evaporation. The expansion continues from here on in a more complex manner since vapour and liquid phase are in close interaction. Additionally, the velocities rise due to evaporation and may reach, given a certain pressure difference between in- and outlet, the magnitude of speed of sound of the used refrigerant. The complex the simulation of such a process might be, the simpler is a capillary's practical use in refrigeration processes. It can be bended, helically spiralled, combined with a heat exchanger to improve the overall performance of the refrigeration cycle, is nearly independent of its position and

Figure 1: Ts - diagram of R600a (isobutane). The grey line represents an adiabatic expansion using a capillary tube for instance.

works without using electronic systems.To reproduce the working principle of a capillary tube numerically, several ways have been invented. Depending on its purpose, the models differ in respect to computational dimensions (0d, 1d), the kind of implementation of multiphase physics (homogeneous model, two fluid model, drift flux model) and the complexity of accounted multiphase phenomena like metastable flow, oil entrainment, choking and behaviour of different flow regimes.

Starting with 0d models, Zhang and Ding (2004) and Hermes *et al.* (2010) presented semi-empirical models based on the work of Yilmaz and Ünal which are explicit in regard to the mass flow. The deviation for a majority (>90 %) of data points lies within a range of ±15 % for R134a and R600a in both cases which justifies its use for cycle simulations. Drawbacks are the low flexibility of the two phase region in respect to the different flow regimes - averaged values for friction and viscosity along the whole two phase domain have to be used.
More sophisticated models have been invented; leading among them in terms of popularity is the homogenous flow model. Park *et al.* (2007), Hermes *et al.* (2008), Guobing and Yufeng (2006), Madsen *et al.* (2005), Bansal and Rupasinghe (1996), Bansal and Wang (2004), Garcia-Valladares *et al.* (2002a, 2002b), Wongwises *et al.* (2000), Wong and Ooi (1995), Xu and Bansal (2002) and others have chosen this model, which is a one-dimensional model, solving the equations of continuity, energy and a simplified momentum-equation for each control volume. The model is capable of accounting for heat transfer through walls, varying two phase friction coefficients and refrigerant properties, which makes this kind of model more accurate than 0d ones. It also leads to better understanding of the expansion process since data at every increment of length can be computed. Despite its better accuracy, an iterative process is necessary to obtain a mass flow at the end. Concerning accuracy, values of mass flow rates differ strongly, dependent on the care of implementation, adiabatic, non-adiabatic conditions and boundary conditions, the range of input parameters and so on, nevertheless it lies between 0d models and more sophisticated two fluid models. Values as guideline can be given by ±5 % average deviation (Guobing and Yufeng, 2006), 5 % relative mean error (Seixlack and Barbazelli, 2009) or an agreement between experimental data and calculated data within ±7 % (Bansal and Wang, 2004). Of course, the comparability of accuracy is hardly given since every author validates against different experimental datasets and implements different submodels (e.g. heat exchanger, helically spiralled tubes, ...).

Other models, like slip models (Escanes *et al.,* 1995), (Garcia-Valladares, 2004), two fluid models (Richter, 1983), (Seixlack and Barbazelli, 2009) or drift flux models (Liang and Wong, 2001), (Wein, 2002) consider one-dimensional hydrodynamic- and thermal non-equilibrium and represent the most complex models in this field of research. The accuracy is expectedly high, Seixlack and Barbazelli (2009) reported a relative mean error of 3.6 % for his two fluid model under choked conditions, whereas his homogeneous model reaches 5 % mean error for mass flow predictions.

Extensive experimental work has been carried out by Melo *et al.* (1994, 1999, 2002), who collected a big amount of data points using R12, R134a and R600a in adiabatic and non-adiabatic capillary tubes. Pressure- and temperature measurements are available not only at the inlet and outlet but also at some points during the expansion. Other measurements have been conducted by Park *et al.* (2007), Madsen *et al.* (2005), Hermes *et al.* (2008), Mittal *et al.* (2010), Fiorelli *et al.* (2002), Vins and Vacek (2009), Kim *et al.* (2002), Jabaraj *et al.* (2006) and other researchers. Motta (2002) published visual studies where he observed R404A / oil flow through an adiabatic glass capillary tube, where the onset of evaporation and the two phase flow regime can be observed.

Very useful reviews have been published by Fang (1999), Khan *et al.* (2009), and Ding (2007) which give a survey about existing publications on capillaries.

2. CAPILLARY TUBE MODEL

Basing on the Equations (1)-(3), a homogeneous capillary tube model has been set up in C programming language using Code::Blocks 8.02 with a GNU GCC compiler (CPU: AMD Athlon 64 3500+). The properties for the refrigerant R600a have been implemented as a set of functions based on the formulations for the thermodynamic properties by Bücker and Wagner (2006). The homogeneous model provides the possibility to implement a heat exchanger and proved to be a solid starting base for capillary tube investigations. The advantages of a numerically simple and stable scheme compared to two fluid models outweigh the drawbacks of being dependent on empirical correlations and mean properties for viscosity and friction. Starting from conservation equations for mass, momentum and energy in its general form (Equations (1)-(3)), a set of simplified equations (Equations (4)-(6)) can

be derived after applying the below-mentioned simplifications. For implementation in a numerical scheme, these equations have been discretized (Equations (7)-(9)) to work on a one-dimensional grid. All variables are listed in the nomenclature section.

continuity:

$$\frac{\partial \rho}{\partial t} + \frac{\partial (\rho \cdot u)}{\partial z} = 0 \tag{1}$$

momentum:

$$\frac{\partial (\rho \cdot u)}{\partial t} + \frac{\partial \left(\rho \cdot u^2 \right)}{\partial z} = -\frac{\partial p}{\partial z} + \left(\frac{\partial \tau_{xz}}{\partial x} + \frac{\partial \tau_{yz}}{\partial y} + \frac{\partial \tau_{zz}}{\partial z} \right) + \rho \cdot g_z \tag{2}$$

energy:

$$\frac{\partial}{\partial t}\left[\left(\rho\cdot\left(e+\frac{u^2}{2}\right)\right)\right] + \frac{\partial}{\partial z}\left[\left(\rho\cdot u\cdot\left(e+\frac{u^2}{2}\right)\right)\right] = \frac{\partial}{\partial z}\left(-p\cdot u - q\right) + \rho \cdot u \cdot g_z + \dot{q} \tag{3}$$

Simplifications implied in the current model:

- capillary is straight.
- refrigerant behaves as a Newtonian fluid.
- transient behaviour is neglected ($\partial / \partial t = 0$). Based on Hermes *et al.* (2000) the transient terms have minor influence on mass flow.
- no heat transfer between wall and refrigerant and no heat sources (q, $\dot{q} = 0$).

- refrigerant is pure and not contaminated with oil and impurities.
- properties of refrigerant are constant over the cross section (one-dimensional assumption).
- constant wall roughness and diameter over the length.

simplified equations:

$$\frac{\partial (\rho \cdot u)}{\partial z} = 0 \tag{4}$$

$$\frac{\partial \left(\rho \cdot u^2 \right)}{\partial z} = -\frac{\partial p}{\partial z} + f_w + \rho \cdot g_z \tag{5}$$

$$\frac{\partial}{\partial z}\left[\left(\rho\cdot u\cdot\left(h+\frac{u^2}{2}\right)\right)\right] = \rho \cdot u \cdot g_z \tag{6}$$

discretized equations:

$$\left[\rho \cdot u\right]^{i+1} - \left[\rho \cdot u\right]^{i} = 0 \tag{7}$$

$$\left[\rho \cdot u^2\right]^{i+1} - \left[\rho \cdot u^2\right]^{i} = -\left[p\right]^{i+1} + \left[p\right]^{i} + \overline{\Delta p} + \Delta z \cdot \rho \cdot g_z \tag{8}$$

$$\left[h + \frac{u^2}{2}\right]^{i+1} - \left[h + \frac{u^2}{2}\right]^{i} = \Delta z \cdot g_z \tag{9}$$

The frictional pressure drop in Equation (8) is denoted as $\overline{\Delta p}$ which stands for the pressure loss over the length of one element and is computed by multiplication of an empirically determined friction factor ("Darcy- or "Darcy-Weisbach friction factor") with the ratio of length to diameter and the dynamic pressure (Equation 10). Equation (11) states the implicit correlation for the friction factor according to Colebrook (Wongwises *et al.* 2000). Care has to be taken to meet the conditions for the correlations (e.g. range of Reynolds number, range of relative roughness, shape of the cross section, ...).

$$\overline{\Delta p} = \overline{\lambda} \cdot \frac{\Delta z}{D} \cdot \frac{\overline{\rho} \cdot \overline{u}^2}{2} \tag{10}$$

$$\sqrt{\frac{1}{\lambda}} = 2 \cdot \log\left(\frac{2.51}{Re \cdot \sqrt{\lambda}} + \frac{k}{D \cdot 3.72}\right) \tag{11}$$

3. CELL DISTRIBUTION AND EMPIRICAL CORRELATIONS

Due to the high gradients at the end of the capillary tube, the spatial resolution was tuned by decreasing the size of the increments. At the same time, it was tried not to increase the cell size at the inlet of the capillary tube since the position of the point of evaporation may be of interest if one deals with metastable flow models and evaporation delay. Equation (12) was used to create such a nodal distribution that the pressure drop per cell gets lower when approaching the end of the capillary even under choked flow conditions. This measure turned out to improve convergence when adjusting the mass flow in order to meet the outlet boundary condition with a numerical accuracy up to a few Pascal. Two parameters, α, β are chosen to shape the function accordingly, each of them is varied in Figure 3 to show the effects on the distribution of cell length over the total length of the capillary.

$$\Delta z(i) = L \cdot \left(\alpha^{\tan\left(\frac{\beta}{100} \cdot \frac{\pi}{2} \cdot \frac{i}{d}\right)}\right)^{-1} \Bigg/ \sum_{i=1}^{i=d}\left(\alpha^{\tan\left(\frac{\beta}{100} \cdot \frac{\pi}{2} \cdot \frac{i}{d}\right)}\right)^{-1} \tag{12}$$
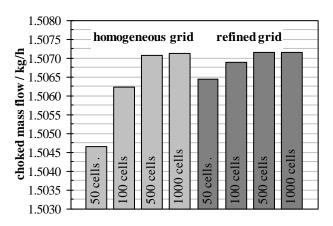
Figure 2: Comparison of choked mass flow rates.

Although the parameters have to be adapted if the mesh size changes drastically, it keeps the total pressure drop per cell in the same order of magnitude. In Figure 2 the choked mass flow is computed using different combinations of grids applying the same boundary conditions. Light grey is on a grid with equally distributed cells, dark grey symbolizes results with a grid using Equation (10) with $\alpha = 1.1$ and $\beta = 99$. It can be seen that fewer cells with advantageous distribution lead to similar mass flow rates as applying homogeneously distributed cells. For instance, no difference can be observed (i.e. the fourth position after the decimal place in mass flow remains unchanged, kg/h as unit of measurement) between a 500- and a 1000-cell refined grid. This leads to the assumption that no significant change in mass flow rate can be expected when the calculation is done with a higher number of cells. An error of 0.05 % compared to the case of a 1000-cell refined grid occurs using 50 cells, which is less than the error which arises using 100 cells on a homogeneous grid. This matter may be of no importance when simulation is compared with experimental results since deviations of ±10 % in mass flow for the vast bulk of data under choked flow conditions are commonly reported values, but it is of importance when calculation speed is expected to be high. The speed of a single iteration over the capillary tube correlates with the total number of cells, so halving them without loss of accuracy doubles the speed for calculating the mass flow rate.
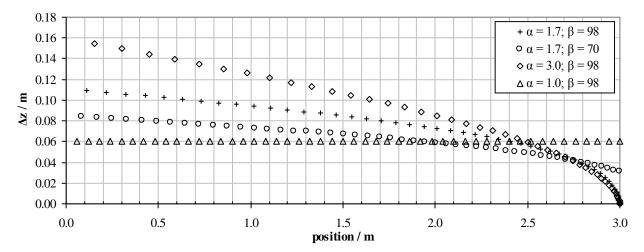

Figure 3: Mesh, generated by equation (12). The settings $\alpha = 1.1$ and $\beta = 99$ were used together with 200 cells for all computations in this work. Here, parameter variations of α and β are shown using a 50-cell grid.

Figure 3 shows the length of cells at the corresponding position of a capillary tube. The case where $\alpha = 1.0$ (irrespective of the value of β) displays the homogeneous case, all other variations lead to a more or less refined grid. The horizontal spacing between the points also indicates the cell length. Concerning the pressure drop, different correlations have been tested. Among them are correlations for the friction factor like by Churchill and Colebrook in combination with two phase viscosities gained by correlations after Akers, Beattie & Whalley, Ciccitti, Davidson, Dukler, Isbin, Lin, Mc Adams and Owen (Dias and Gasche, 2008), (Wong and Oii, 1995). Also, two phase multipliers by Lin, Friedel and Lockhart-Martinelli have been tested (Field and Hrnjak, 2007), (Wongwises *et al.*, 2000). The combination which leads to the least deviations from a set of measurements by Melo *et al.* (1999) is Colebrook's friction coefficient for the liquid phase, Churchill's friction factor for vapour phase and Friedel's two phase multiplier for two phase flow.
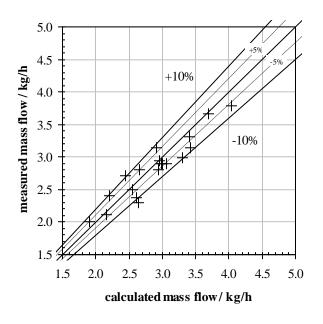
Figure 4: Friction coefficients: Colebrook (liquid) and Churchill (vapour). Two phase multiplier: Friedel.

These settings were used for all further computations. All relaxation parameters could be set to 1 without affecting the stability of the program for the worse. Choked flow is achieved when the set of equations are on the limit of fulfillment in the last cell. This fact turned out to be a major issue since the mathematical model becomes instable when the mass flow is raised beyond the critical mass flow, which makes iterations, in particular mass flow iterations to reach a certain outlet pressure, very instable. Numerically this is mainly accomplished by Regula-Falsi- or secant-methods, which were found to be the most stable way and are preferred over Newton-methods. Choked flow conditions also could be found by comparing the velocity at the end of each cell with the speed of sound computed from property tables. A word, too, about convergence criteria. The iteration within a cell is converged when the changes in pressure from one iteration to another are below 10^{-5}, which corresponds to a few Pascal. The same level applies for the choked flow iteration, where the relative error in mass flow must be less than 10^{-5}. For the final outlet pressure iteration, the relative error in outlet pressure is below $5 \cdot 10^{-5}$, which corresponds to an absolute error of less than 10 Pa, taking 2 bars as desired outlet pressure.

4. PARAMETER STUDIES

The aim of this chapter is to identify the main influences on the mass flow rate, which constitutes a key parameter of a cycle simulation. The capillary tube, together with the other components, affects the mass flow in a physical cooling cycle and so should the corresponding models with respect to the boundary conditions. First, the thermodynamic state of the refrigerant are varied and the dependence of the mass flow is shown in Figure 5. In (a) and (b) the outlet pressure is plotted against the mass flow rate. Choking can be observed in both cases (bold lines) where the pressure at the outlet is below 2 bars. The same graph is shown for different degrees of subcooling (a) and inlet pressures (b). Furthermore, the correlation between subcooling (c) or inlet pressure (d) and mass flow rate is shown, which turns out to behave more linearly than variations of outlet pressure. All plots from Figure 5 have in common that they originate from the same boundary conditions and show deviations of one parameter. Is this behaviour depending on the specific boundary conditions or can a general conclusion be drawn?

To find an answer to this question and to determine which parameters have the biggest or smallest influence, a different kind of parameter variation should lead to clarification. Therefore, a high number of different boundary conditions, which may occur during operation, are applied on a capillary tube of constant geometry. Table 1 shows the range of variations. With each of these sets of values, mass flow rates can be computed for each specific boundary condition. Then, one parameter is chosen (e.g. subcooling at the inlet) and varied by 10 % of its value. The same procedure (calculating mass flow rates) is carried out again, this time with the one parameter slightly changed. This leads to a change in mass flows in every one of the new points. These mass flows compared with the "standard characteristic field" may be expressed by means of an averaged value and a standard deviation - so it is in Figure 6. This figure tells for instance, that an increase of 10 % in diameter leads to an average increase in mass flow rate by 1.13 kg/h regarding the operating range given in table 1. When looking at the influence of pressure in this diagram, one may notice a high standard deviation. This can be explained due to the highly nonlinear influence of pressure, as can be seen in Figure 5 (a, b).
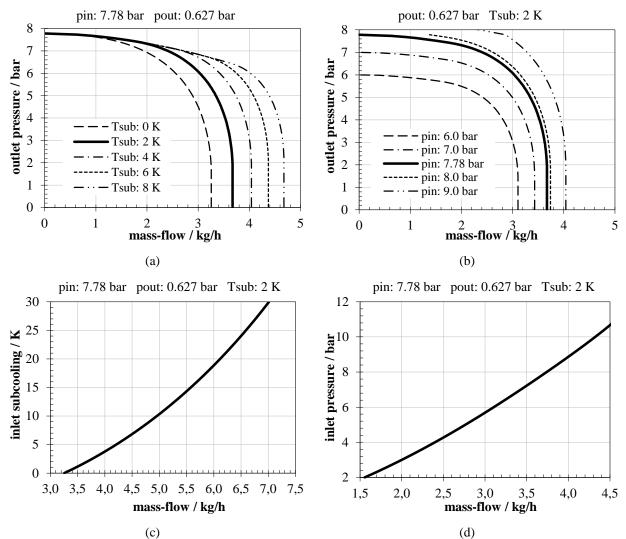
(a)

(b)

(c)

(d)

Figure 5: Standard values for all bold graphs are: p_{in} = 7.78 bar, p_{out} = 0.627 bar, T_{sub} = 2K. One parameter varies.

Table 1: Values for standard-case and variations. The notation 3:1:10 means 3 up to 10 with step-size of 1.

parameter	L	D	k	p_{in}	p_{out}	T_{sub}	φ	friction	grid
unit	m	mm	μm	bar	bar	K	°	-	-
standard-value	3.0	1.0	0.750	3:1:10	3:1:10	0.5, 1:1:15	horizontal	Friedel	200 cells $α$=1.1; $β$=99
min-value	2.7	0.9	0.675	3:1:10 - 10%	3:1:10 - 10%	0.5, 1:1:15 - 10%	+10° (≈ +0.5 m)	Bittle&Pate Dukler	200 cells homogenous
max-value	3.3	1.1	0.825	3:1:10 + 10%	3:1:10 + 10%	0.5, 1:1:15 + 10%	-10° (≈ -0.5 m)		

This denotes that the influence of pressure on mass flow rate highly depends on the rest of the boundary conditions. Although the standard deviation is a common value for statistical analysis, here, in the case of pressure it makes only sense partially since in no test case occurs a rise in mass flow when the outlet pressure is raised, as it does in Figure 6. Else, from Figure 6 can be concluded, that if the mean change in mass flow rate is high, the influence of the parameter responsible for this deviation is high and it has to be treated with care. Also, parameters which show a comparably small difference in the mass flow rate may be neglected for future computations. In this case it can be assumed, that the influence of the wall roughness and the inclination is rather small and that diameter, length, thermodynamic boundary conditions as well as the appropriate choice of friction law are of primary interest.
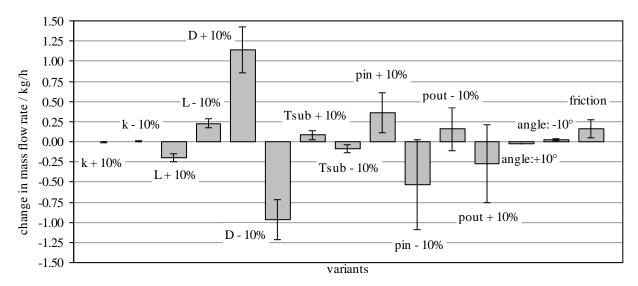
Figure 6: Mean and standard deviations in mass flow rate due to changes of boundary conditions. 704 points were taken for this sensitivity study.

One can play the game in another way as well, it is, finding the absolute deviation in single parameters to account for a predetermined change in mass flow rate, let's say a decrease by 0.1 kg/h. Taking reference-values for geometry and thermodynamic boundary conditions, the sensitivity can be seen in table 2. Here, length and inclination can be measured so accurately (millimetres and degree, respectively) that any measuring error wouldn't affect the mass flow computation. More critical turn out to be temperature and pressure. According to this table, an accuracy of about ±0.25 K for temperature and ±0.15 bar for inlet pressure leads both to an error of 0.1 kg/h in mass flow rate.

Table 2: Ways to lower the mass flow by 0.1 kg/h by changing one parameter only.

parameter	deviation	reference
L	+ 15 cm	3 m
D	- 0.01 mm	1 mm
k	+ 2.75 μm	0.75 μm
φ	+ 90°	0°
p_{in}	- 0.3 bar	7.78 bar
p_{out}	none	0.627 bar
T_{sub}	- 0.5 K	2 K

The outlet pressure doesn't influence the result in this case, since choked conditions prevail and therefore a variation in outlet pressure has no effect on the mass flow rate. The surface roughness and the diameter are both hard to measure, and especially the accurate knowledge of the diameter should be given. A change by one hundredth of a millimetre in diameter shifts the mass flow by 0.1 kg/h. The problem which results from this awareness is that it has to be guaranteed that the inner diameter of a capillary tube has to be within ±5 μm over the whole length if errors in the order of 0.1 kg/h should be avoided. Also the specification of the manufacturer concerning inner diameter should be verified if possible. The surface roughness matters as well, but since the process of drawing, which is applied to capillary tubes, can be controlled in such a way that the surface roughness can be usually maintained between 0.7 μm and 1.5 μm, this issue is regarded to be less important than accurate temperature-, pressure- or diameter-data. Additionally, it has to be mentioned, that the errors in mass flow resulting from uncertainties of single input parameters may sum up and therefore the accuracy of measurement should be adapted correspondingly.

5. CONCLUSION

In the course of this study homogeneous adiabatic capillary tube model is derived. The model is validated against experimental data under consideration of a special cell distribution which leads to better resolution of gradients at the end of the capillary tube. The responsivity of mass flow rate to changes in boundary conditions is investigated, and it is found that the main parameters are diameter, inlet- and outlet pressure as well as the choice of an appropriate friction model. Gravity and roughness of the surface only play a minor role whereas exact knowledge of length and subcooling of the refrigerant seem to be of importance, but, considering the rather high accuracy of measurements for length and temperature, resulting errors can be kept low. Great care should be taken in the choice of the inner diameter of a capillary tube. Given mean deviations of ±1 kg/h induced by ±0.1 mm difference in diameter, one should check the nominal diameters of the manufacturers and if necessary apply own measurements.

NOMENCLATURE

d	total number of cells	(-)		**Superscripts**		
D	inner diameter	(m)		i	cell number	(-)
e	specific energy	(J/kg)		-	cell average	(-)
f_w	wall friction per volume	(N/m^3)				
g	gravitational acceleration	(m/s^2)		**Subscripts**		
h	enthalpy	(J/kg)		in	inlet	(-)
k	absolute surface roughness	(m)		out	outlet	(-)
L	capillary length	(m)		sub	subcooling	(-)
p	pressure	(Pa)				
q	heat flux per unit area	(W/m^2)		**Greek symbols**		
$\dot{q}$	heat source per unit volume	(W/m^3)		α	grid parameter	(-)
Re	Reynolds number	(-)		β	grid parameter	(-)
t	time	(s)		Δ	increment	(-)
T	temperature	(K)		λ	friction coefficient	(-)
u	velocity (in z direction)	(m/s)		ρ	density	(kg/m^3)
x	length in x-direction	(m)		τ	shear stress	(N/m^2)
y	length in y-direction	(m)		φ	angle of inclination	(°)
z	length in z-direction	(m)				

REFERENCES

Bansal, P. K., Rupasinghe, A. S., 1996, An empirical model for sizing capillary tubes, *International Journal of Refrigeration,* vol. 19, no. 8: p. 497-505.

Bansal, P. K., Wang, G., 2004, Numerical analysis of choked refrigerant flow in adiabatic capillary tubes, *Applied Thermal Engineering,* vol. 24: p. 851-863.

Bücker, D., Wagner W., 2006, Reference Equations of State for the Thermodynamic Properties of Fluid Phase n-Butane and Isobutane, *Journal of Physical and Chemical Reference Data,* vol. 35, no. 2: p. 929-1019.

Dias, J. P., Gasche, J., 2008, Analysis of mean viscosity correlations on numerical simulation of the oil/refrigerant R134a mixture two-phase flow in a small diameter tube, 5th European Thermal-Sciences Conference, The Netherlands.

Ding, G. L., 2007, Recent developments in simulation techniques for vapour-compression refrigeration systems, *International Journal of Refrigeration,* vol. 30: p. 1119-1133.

Escanes, F., Perez-Segarra, C. D., Oliva, A., 1995, Numerical simulation of capillary-tube expansion devices, *International Journal of Refrigeration,* vol. 18: p. 113-122.

Fang, X., 1999, Advances in fixed-area expansion devices, Technical report, Air Conditioning and Refrigeration Center, University of Illinois.

Field, B. and Hrnjak, P. , 2007, Two-Phase Pressure Drop and Flow Regime of Refrigerants and Refrigerant-Oil Mixtures in Small Channels, Technical report, Air Conditioning and Refrigeration Center, University of Illinois, USA.

Fiorelli, F. A. S., Huerta, A. A. S. and Silvares, O. d. M., 2002, Experimental analysis of refrigerant mixtures flow through adiabatic capillary tubes, *Experimental Thermal and Fluid Science,* vol. 26: p. 499-512.

Garcia-Valladares, O., Perez-Segarra, C. and Oliva, A., 2002a, Numerical simulation of capillary-tube expansion devices behaviour with pure and mixed refrigerants considering metastable region. Part I: mathematical formulation and numerical model, *Applied Thermal Engineering*, vol. 22: p. 173-182.

Garcia-Valladares, O., Perez-Segarra, C. and Oliva, A., 2002b, Numerical simulation of capillary-tube expansion devices behaviour with pure and mixed refrigerants considering metastable region. Part II: experimental validation and parametric studies, *Applied Thermal Engineering*, vol. 22: p. 379-391.

Garcia-Valladares, O., 2004, Review of numerical simulation of capillary tube using refrigerant mixtures, *Applied Thermal Engineering,* vol. 24: p. 949-966.

Guobing, Z., Yufeng, Z. 2006, Numerical and experimental investigations on the performance of coiled adiabatic capillary tubes, *Applied Thermal Engineering,* vol. 26: p. 1106-1114.

Hermes, C. J. L., Melo, C., Negrao, C. O. R., Mezavila, M. M., 2000, Dynamic simulation of HCF-134a flow through adiabatic and non-adiabatic capillary tubes, International Refrigeration and Air Conditioning Conference at Purdue, West Lafayette, USA, pp. 295–303.

Hermes, C. J. L., Melo, C., Goncalves, J. M., 2008, Modeling of non-adiabatic capillary tube flows: A simplified approach and comprehensive experimental validation, *Int. Journal of Refrigeration,* vol. 31: p. 1358-1367.

Hermes, C. J. L., Melo, C., Knabben, F. T., 2010, Algebraic solution of capillary tube flows Part I: Adiabatic capillary tubes, *Applied Thermal Engineering,* vol. 30: p. 449-457.

Jabaraj, D., Kathirvel, A. V. and Lal, D. M., 2006, Flow characteristics of HFC407C/HC600a/HC290 refrigerant mixture in adiabatic capillary tubes, *Applied Thermal Engineering,* vol. 26: p. 1621-1628.

Khan, M. K., Kumar, R. and Sahoo, P. K., 2009, Flow characteristics of refrigerants flowing through capillary tubes – A review, *Applied Thermal Engineering,* vol. 29: p. 1426-1439.

Kim, S. G., Kim, M. S. and Ro, S. T., 2002, Experimental investigation of the performance of R22, R407C and R410A in several capillary tubes for air-conditioners, *International Journal of Refrigeration,* vol. 25: p. 521-531.

Liang, S. M. and Wong, T. N., 2001, Numerical modeling of two-phase refrigerant flow through adiabatic capillary tubes, *Applied Thermal Engineering,* vol. 21: p. 1035-1048.

Madsen, K. B., Poulsen, C. S., Wiesenfarth, M., 2005, Study of capillary tubes in a transcritical CO2 refrigeration system, *International Journal of Refrigeration,* vol. 28: p. 1212-1218.

Melo, C., Ferreira, R., Boabaid Neto, C. B., Goncalves, J. M, Pereira, R. H. and Thiessen, M. R., 1994, Evaluation of HC-600a, HFC-134a and CFC-12 mass flow rates through capillary tubes, New Applications to Reduced Global Warming and Energy Consumption Conference, Hannover, Germany, May 10-13, p. 621-630.

Melo, C., Ferreira, R., Neto, C. B., Goncalves, J. M., Mezavila, M., 1999, An experimental analysis of adiabatic capillary tubes, *Applied Thermal Engineering,* vol 19: p. 669-684.

Melo, C., Vieira, L. A. T. and Pereira, R. H., 2002, Non-adiabatic capillary tube flow with isobutane, *Applied Thermal Engineering,* vol. 22: p. 1661-1672.

Mittal, M., Kumar, R. and Gupta, A., 2010, An experimental study of the flow of R-407C in an adiabatic helical capillary tube, *International Journal of Refrigeration,* vol. 33: p. 840-847.

Park, C., Lee, S., Kang, H., Kim, Y., 2007, Experimentation and modeling of refrigerant flow through coiled capillary tubes, *International Journal of Refrigeration,* vol. 30: p. 1168-1175.

Peixoto, R. A. and Bullard, C. W., 1994, A Design Model for Capillary Tube-Suction Line Heat Exchangers, Technical report, Air Conditioning and Refrigeration Center, University of Illinois, USA.

Richter, H. J., 1983, Separated two-phase flow model: application to critical two-phase flow, *International Journal of Multiphase Flow,* vol. 9, no. 5: p. 511-530.

Seixlack, A., Barbazelli, M., 2009, Numerical analysis of refrigerant flow along non-adiabatic capillary tubes using a two-fluid model, *Applied Thermal Engineering,* vol. 29: p. 523-531.

Wein, M., 2002, Numerische Simulation von kritischen und nahkritischen Zweiphasenströmungen mit thermischen und fluiddynamischen Nichtgleichgewichtseffekten, PhD thesis, Technischen Universität Dresden, Germany.

Vins, V. and Vacek, V., 2009, Mass flow rate correlation for two-phase flow of R218 through a capillary tube, *Applied Thermal Engineering,* vol. 29: p. 2816-2823.

Wong, T. N. and Ooi, K. T., 1995, Refrigerant flow in capillary tube: an assessment of the two-phase viscosity correlations on model prediction, *International Communications in Heat and Mass Transfer*, vol. 22, no. 4: p. 595-604.

Wongwises, S., Chan, P., Luesuwanatat, N. and Purattanarak, T., 2000, Two-phase separated flow model of refrigerants flowing through capillary tubes, *International Journal of Heat and Mass Transfer*, vol. 27: p. 343-356.

Xu, B. and Bansal, P. K., 2002, Non-adiabatic capillary tube flow: a homogeneous model and process description, *Applied Thermal Engineering,* vol. 22: p. 1801-1819.

Zhang, C., Ding, G., 2004, Approximate analytic solutions of adiabatic capillary tube, *International Journal of Refrigeration,* vol. 27: p. 17-24.

ACKNOWLEDGEMENT